



Design the DLQR Digital Controller to Stabilize the Trajectory for the UAV

Nguyen Thanh Phong¹, Le Ngoc Giang^{2}, Tran Dang Cao Thien³*

¹Master, Lecturer, Faculty of Fundamental Technics, AD-AF Academy of Viet Nam, Ha Noi, Vietnam

²Doctor, Head of Department, Faculty of Fundamental Technics, AD-AF Academy of Viet Nam, Ha Noi, Vietnam

³Graduate Student, SMS-1, AD-AF Academy of Viet Nam, Ha Noi, Vietnam

* Email: lengocgianglinh@gmail.com

ABSTRACT

Orbital stabilization for fixed-wing unmanned aerial vehicles is a complex task. With the same set angle value, but the actual flight trajectory results are different in different conditions of altitude, airspeed, temperature, dynamic pressure... The control of fixed-wing unmanned aircraft includes many channels, namely the pitch angle controller, roll angle controller, yaw angle controller. They are usually designed using traditional PID control methods. However, in order to gain a tactical advantage, modern fighters are often geared toward maneuvers outside the linear region, so a more effective approach is to design the full-state Linear Quadratic Regulator (DLQR). This is an important basis for the actualization of the orbital-stabilized DLQR digital controller for fixed-wing unmanned aerial vehicles. The simulation results show the effectiveness and sustainability of this control strategy even in the presence of aerodynamic torque disturbances and parametric instability.

Keywords: DLQR controller, fixed-wing unmanned aircraft, flight trajectory

1. Introduction

Unmanned aerial vehicle (UAV) are gradually becoming popular for civil and military purposes. Controlling the fixed-wing unmanned aerial vehicle to stabilize its trajectory plays a particularly important role. In order for the UAV to perform well in complex environments, various control algorithms are required [1]. Nonlinear control [2], Backstepping control [3], sliding control [4], fuzzy control, and Noron network [5] are examples of modern control theory studies that can be applied to UAVs. Studies have shown many advantages to modern control methods. However, their practical applicability is very low due to complicated calculations and the high cost of the controller.

The terms in Figure 1 are as follows:

Roll - Longitudinal axis; Pitch - Lateral axis; Yaw - Vertical axis;

Aileron - are a primary flight control surface which control movement about the longitudinal axis of an aircraft;

* Corresponding author: *Le Ngoc Giang*. Tel.: +84969896136

E-mail address: lengocgianglinh@gmail.com

Elevator - are flight control surface, usually at the rear, to control the aircraft's pitch through the angle of attack and the lift of the wing;

Rudder - is a primary flight control surface that governs an aircraft's rotation around its vertical axis is referred to as "Yaw". The rudder attached to the vertical stabilizer or fin's trailing edge.

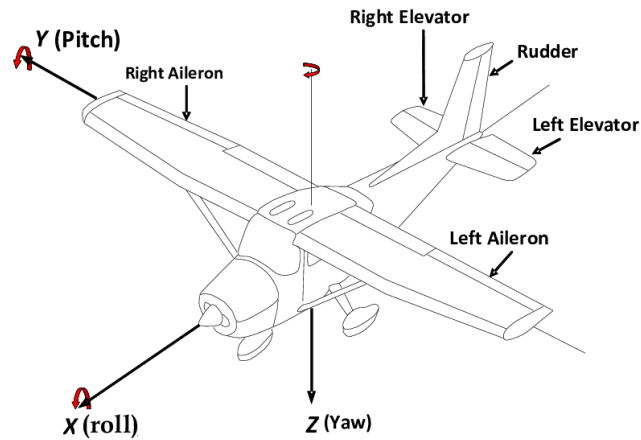


Fig.1 - Control mechanisms of the Ultra Stick 25e UAV [9]

In many studies, the control of fixed-wing drones uses traditional PID controllers [6]. The linear PID controller has a simple structure, easy to implement, easy to calculate and design because it only needs to adjust 3 parameters K_p , K_i , K_d . However, the development of today's air force needs to reduce radar detection, high airspeed, strong maneuverability... That has created challenges in improving accuracy when design the flight controls of the aircraft. In fact, the fixed-wing unmanned aircraft is a strong nonlinear object, subject to many environmental influences such as temperature, pressure, altitude, wind... Therefore, linear PID controllers may not be able to meet the required criteria. In this paper, the authors propose to use the DLQR Linear Quadratic Regulator digital controller, replacing the PID controller and modern controllers. This is a controller with an uncomplicated structure that still ensures the efficiency and sustainability of modern control methods.

2. Design method of the DLQR controller

The design method of a linear quadratic optimal digital controller is evaluated as a promising design tool. The mathematical basis of this design method is as follows [7]:

For a discrete linear object described by the equation of state

$$x(k+1) = A_d x(k) + B_d u(k) \quad (1)$$

In which

$$x(k) = [x_1(k), x_2(k), \dots, x_n(k)]^T: \text{state vector}$$

$$u(k) = [u_1(k), u_2(k), \dots, u_m(k)]^T: \text{control signal vector}$$

The goal is to find the control signal $u(k)$ that will allow the system to meet the quadratic quality criterion function.

$$J(u) = \frac{1}{2} \sum_{k=0}^{\infty} [x^T(k) Q x(k) + u^T(k) R u(k)] \quad (2)$$

The optimum control signal: $u^*(k) = -Kx(k)$

In which: $K = [B_d^T P B_d + R]^{-1} B_d^T P A_d$

P is a positive semi-definite solution of the algebraic Riccati Equation.

$$P = A_d^T (P - P B_d (B_d^T P B_d + R)^{-1} B_d^T P) A_d + Q \quad (3)$$

The minimum value of the quality indicator function: $J_{min} = x^T(0) P x(0)$

3. Identification of the longitudinal motion equation of the UAV Ultra Stick 25e

3.1. A priori model of the longitudinal motion of a UAV according to angle of attack

Longitudinal motion is the reciprocating motion of the aircraft along the Ox and Oy axes and the rotation of the aircraft around the Oz axis. In other words, longitudinal motion is the movement that the aircraft makes in the vertical plane along the plane's axis according to the coordinates x, altitude H, and pitch angle θ .

The a priori model of the longitudinal motion of the UAV according to pitch angle is a second-order oscillator with a structural diagram as shown in Figure 2:

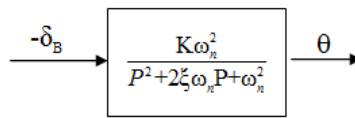


Fig.2 - A priori model of the longitudinal motion of the UAV according to pitch angle

3.2. Method to identify the dynamic model for the second-order oscillator through impulse response

To identify the dynamic model, we excite the input as a unit pulse function and measure the output response. As shown in Figure 3, the impulse response of the second-order oscillator is $g(t)$.

$$g(t) = \frac{dh(t)}{dt} = L^{-1} \{W(p)\} = K \cdot \frac{\omega_n^2}{\beta} \cdot e^{-\alpha \cdot t} \cdot \sin \beta \cdot t$$

$$g(t) = K \cdot (\omega_n \cdot \omega_n / \beta) \cdot g_1(t) \cdot g_2(t)$$

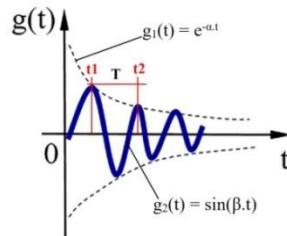


Fig.3 - The impulse response of the second-order oscillator

We see that the impulse response of the second-order oscillator has the form of a damped oscillation. The amplitude of the oscillation decreases with an exponential law.

$$g_1(t) = e^{-\alpha \cdot t}$$

The impulse response will oscillate according to the law of sine functions.

$$g_2(t) = \sin(\beta \cdot t)$$

- **Calculate β :** Based on the expression and graph of $g(t)$, we see that the response's angular frequency is:

$$\beta = 2 \cdot \pi \cdot f = 2 \cdot \pi / T \tag{4}$$

By observing the impulse response, we can determine T, then calculate $\beta = 2 \cdot \pi / T$. In which: $T = t_1 - t_2$

So to calculate β , we only need to determine t_1, t_2 . Where t_1 is the time when the impulse response is maximal for the first time; t_2 is the time when the impulse response reaches its maximum for the second time;

- **Calculating α :** Looking at Figure 3, at time $t_1, t_2, g_2(t) = \sin(\beta.t)$ reaches the Max value ie:

$$g_2(t_1) = \sin(\beta.t_1) = 1; \quad g_2(t_2) = \sin(\beta.t_2) = 1$$

Therefore:

$$g(t_1) = K.(\omega_n. \omega_n / \beta). e^{-\alpha.t_1};$$

$$g(t_2) = K.(\omega_n. \omega_n / \beta). e^{-\alpha.t_2};$$

$$g(t_1)/g(t_2) = e^{\alpha.(t_2-t_1)};$$

We deduce that:

$$\alpha = \ln [g(t_1)/g(t_2)] / (t_2 - t_1) \tag{5}$$

- **Calculating ξ and ω_n**

$$\alpha = \xi. \omega_n; \quad \beta = \omega_n. \sqrt{1 - \xi^2}$$

Set $m = \alpha / \beta = \xi / \text{sqrt}(1 - \xi^2),$

We deduce that:

$$\xi = | \text{sqrt}[m^2 / (1 + m^2)] |, \quad \omega_n = \alpha / \xi \tag{6}$$

- **Calculating K**

$$K = g(t_1) / [(\omega_n. \omega_n / \beta). e^{-\alpha.t_1}] \tag{7}$$

3.3. Identification of the longitudinal motion model of the UAV through impulse response

- Collecting the model's impulse response measurement results:

With the Stick25e fixed-wing Ultra UAV, the specifications are given in Table 1.

Table 1. Specifications of Ultra Stick25e UAV

Quantity	Notation	Value	Unit
Mass	m	1.959	kg
Wing bowstring	B	1.27	m
Wing area	S	0.31	m ²
The average aerodynamic bowstring	\bar{c}	0.25	m
Lift coefficient	C_L	0.458	-
Drag coefficient	C_D	0.0434	-
Thrust coefficient	C_T	0.75	-
Torque coefficient	C_M	0.86	-
Normal coefficient	C_w	1.37	
Flight speed	U	13-18	m/s
Air density	ρ	0.0013	g/m ³
Minimum speed	V_{\min}	10	m/s
Maximum speed	V_{\max}	25	m/s

To measure the impulse response, we take the input action as a unit pulse and measure the output. Measurement results of 256 values of impulse response:

$$G=[0.01459;0.09223;0.16487;0.23240;0.29471;.....;0.00903;0.00687;0.00475;0.00268]$$

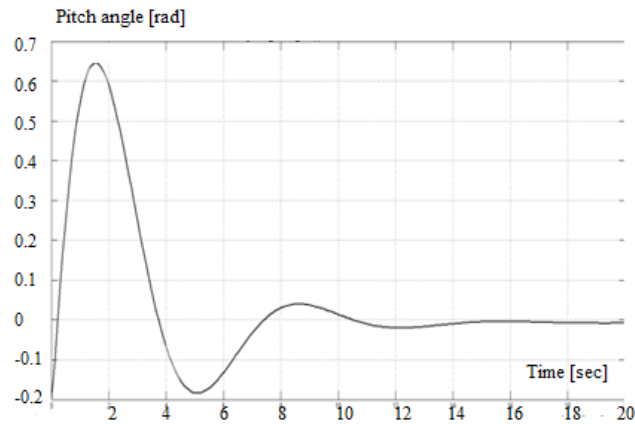


Figure 4. Impulse response of the longitudinal channel of the Stick25e fixed-wing Ultra UAV

On the basis of the algorithm described in Section 3.2, the author has built a tool to identify the longitudinal motion of a UAV through impulse response. Currently, this identification tool is being applied in the measurement practice room at AD-AF Academy. Using the identification tool through impulse response, the author's team has conducted longitudinal motion pattern identification of the fixed-wing Ultra Stick25e UAV. The results of identifying the coefficients of state in the continuous domain of the equation of state describing the longitudinal channel of the Stick25e fixed-wing Ultra UAV are as follows:

$$A = [-0.313 \ 56.7 \ 0; -0.0139 \ -0.426 \ 0; 0 \ 56.7 \ 0];$$

$$B = [0.232; 0.0203; 0];$$

$$C = [0 \ 0 \ 1];$$

$$D = [0];$$

Conduct verification and compare the identification results between the theoretical model and the identification model of the aircraft in longitudinal motion for 3 cases:

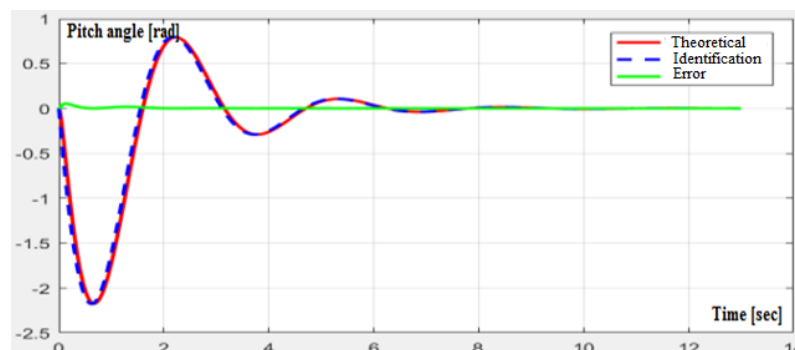


Fig.5 - Results of verification of the identification model with input signal as a unit pulse

- The input is a unit-step function;
- The input is sinusoidal oscillation;
- The input effect is a unit-step function combining sinusoidal oscillations with noise.

It shows that the output response of the theoretical model and the identification model is always close to each other, with a concordance of 99.67%, the final prediction error FPE of $1.96 \cdot 10^{-5}$, and the mean square error MSE of $1.86 \cdot 10^{-5}$.

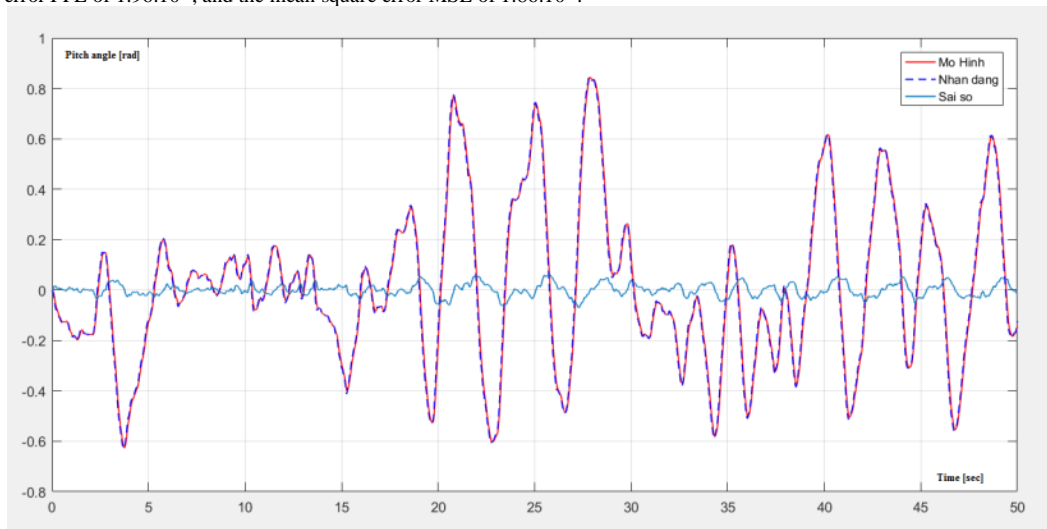


Fig.6 - Verification results of the identification model with a random input signal

3.3. Building a digital controller DLQR for the longitudinal channel of the Stick25e Ultra UAV

The schematic diagram of a state feedback numerical control system is shown in Figure 7, where q-1 is the delay hold; K is the gain matrix; $x = [\alpha, q, \theta]$ is the state vector; θ_{des} is the reference input; δ is the control input; θ is the output vector; A is the system matrix; B is the control matrix; C is the output matrix [8].

With the state feedback law:

$$\delta(k) = \theta_{des}(k) - Kx(k) \tag{8}$$

We have:

$$\begin{cases} x(k+1) = (A - BK)x(k) + B\theta_{des}(k) \\ \theta(k) = Cx(k) \end{cases} \tag{9}$$

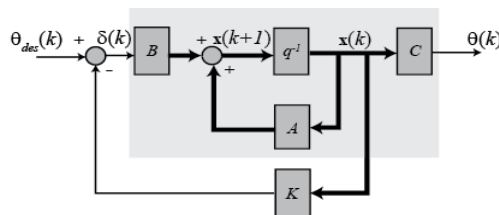


Fig.7 - State feedback digital control system

Design criteria: Over-adjustment is less than 10%; Rise time is less than 2 seconds; The transient time is less than 10 seconds; The setting error is less than 2%.

To design a digital controller, it is necessary to convert the object model to the discrete domain. Select sampling time $T_s = 0.01$ seconds, using a ZOH order holder. The longitudinal motion discrete state-space model of the UAV Ultra Stick 25e is:

$$\begin{bmatrix} \alpha(k+1) \\ q(k+1) \\ \theta(k+1) \end{bmatrix} = \begin{bmatrix} 0.9969 & 0.5649 & 0 \\ -0.0001 & 0.9957 & 0 \\ 0 & 0.5658 & 1 \end{bmatrix} \begin{bmatrix} \alpha(k) \\ q(k) \\ \theta(k) \end{bmatrix} + \begin{bmatrix} 0.0024 \\ 0.0002 \\ 0.0001 \end{bmatrix} [\delta(k)]$$

$$y(k) = \begin{bmatrix} 0 & 0 & I \end{bmatrix} \begin{bmatrix} \alpha(k) \\ q(k) \\ \theta(k) \end{bmatrix} + \begin{bmatrix} 0 \end{bmatrix} \delta(k)$$

To meet the required design quality criteria, select:

$$p = 200; Q = p * C' * C; R = I;$$

The state feedback controller has the following parameters:

$$K = [-0.6633 \quad 249.7299 \quad 13.7945]$$

4. Simulation and evaluation of digital controller DLQR

DLQR controller transient response without compensation:

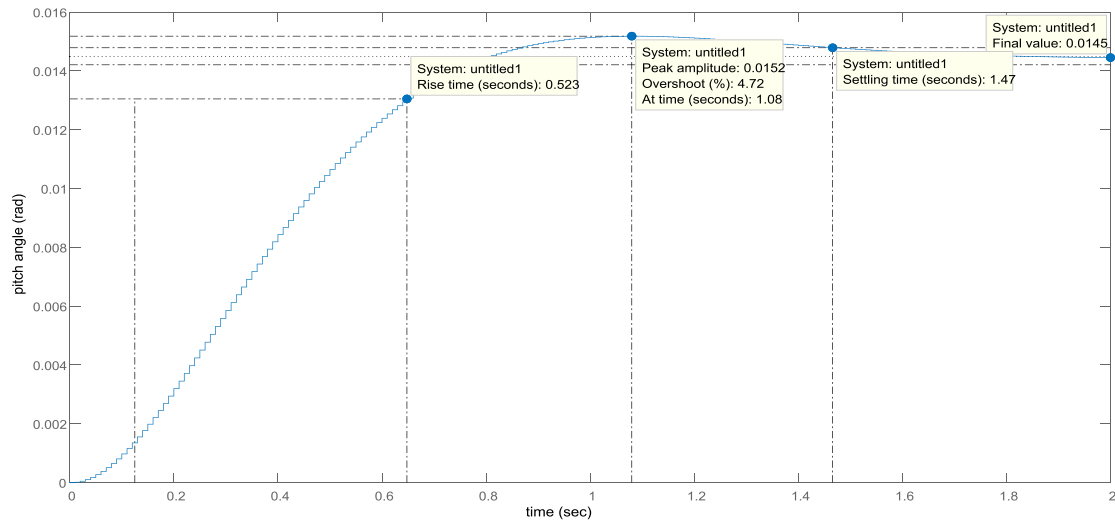


Fig.8 - DLQR controller transient response without compensation

- Overshoot 4.72% less than 10%
- Increment time 0.523 seconds is less than 2 seconds.
- Transition time of 1.47 seconds is less than 10 seconds.

However, the setting error is $0.2 - 0.0145 = 0.1855 = 18.55\%$ greater than 2%. We need to add Nbu compensation at the input as shown in the figure below:

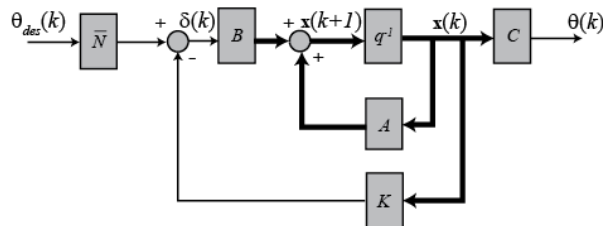


Fig.9 - Diagram of the state feedback digital control system with compensation

The transient response of the DLQR controller with compensation is as shown in Figure 10.

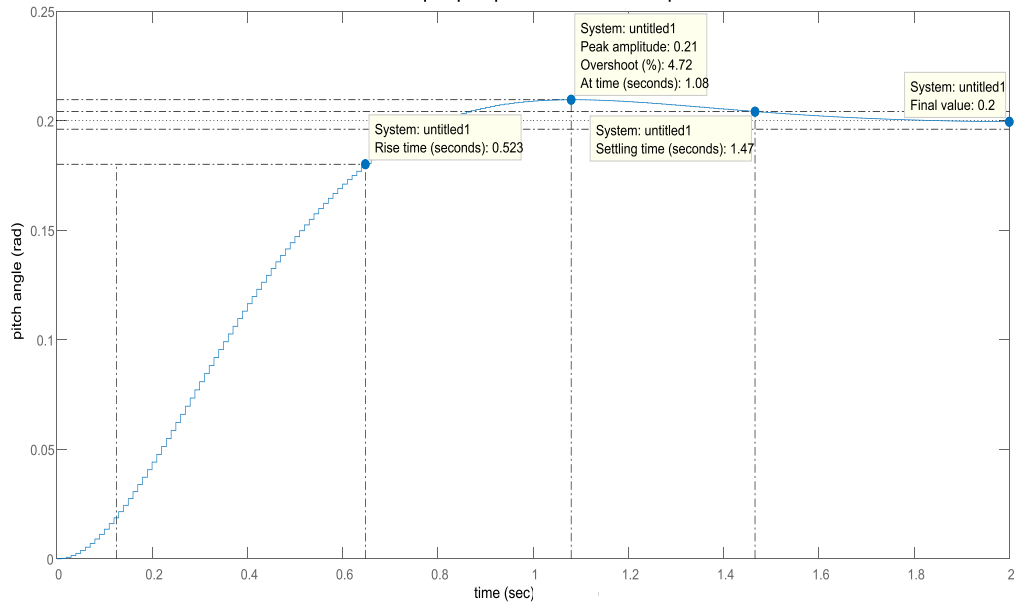


Fig.10 - Transient response of the DLQR controller with compensation

From this figure, we see that the setting error has been completely eliminated, and all design requirements are met.

To consider the role of the controller in the presence of additional noise, suppose we introduce random noise as shown in Figure 11.

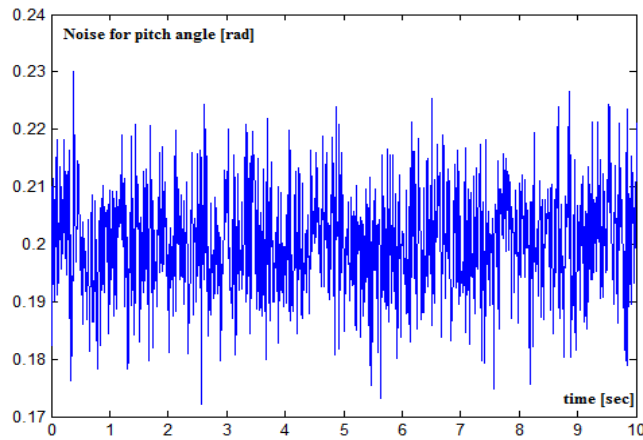


Fig.11 - Impact noise

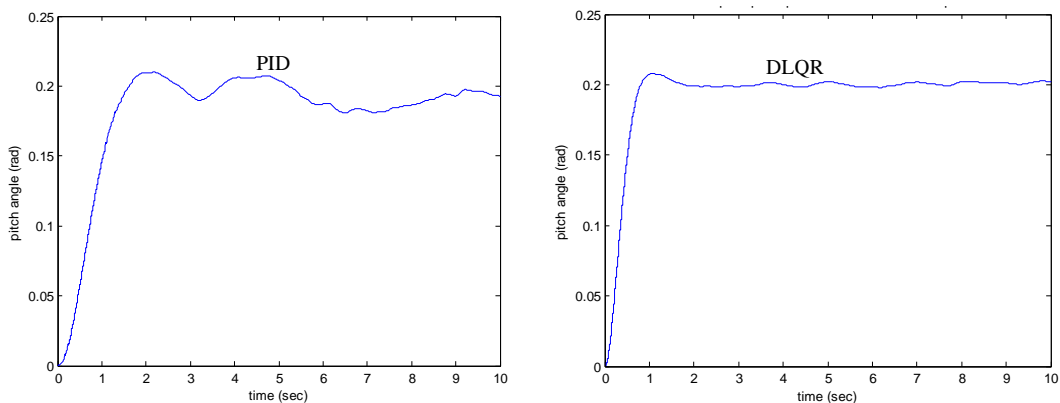


Fig.12 - Transient response of the PID and DLQR controllers when the same noise level is applied

From Figure 12, we can see that when there is an additional impact of noise, the DLQR controller still ensures that it maintains a system that meets all design requirements. However, when the same level of noise is present, the PID controller responds more slowly, and the response fluctuates significantly around the steady-state value.

5. Conclusion

Through the research process "Design the DLQR digital controller to stabilize the trajectory for the UAV", the author has synthesized a DLQR digital controller to stabilize the longitudinal motion trajectory for fixed-wing unmanned aircraft of the Ultra Stick25e type. The simulation results show that the control response is good if the appropriate weight matrices are selected for the DLQR controller. When comparing the efficiency of the two PID and DLQR controllers when having the same noise level, the DLQR controller ensures the system meets all design requirements while the PID controller responds more slowly and fluctuates a lot around the set value.

The research results should be further developed on the basis of the combination of the DLQR controller and Kalman filter, which will be the DLQG controller. The DLQG control applies to both time-invariant linear systems and time-variable linear systems. The application to time-varying linear systems allows the design of linear feedback controllers for unstable nonlinear systems. That is also the wish of the authors, and that will be the direction of future research.

ACKNOWLEDGEMENT

This work is supported by Faculty of Fundamental Technics, AD-AF Academy of Viet Nam.

REFERENCES

- [1]. Kim, J.; Kim, S.; Ju, C.; Son, H.I. (2019). Unmanned aerial vehicles in agriculture: A review of perspective of platform, control, and applications. *IEEE, Vol. 7, pp.105100-105115.*
- [2]. Miroslav K., Ioannis K. (1995). Nonlinear and adaptive control design. *Prentice Hall.*
- [3]. Lee, D.; Ha, C.; Zuo, Z. (2013). Backstepping control of quadrotor-type UAVs and its application to teleoperation over the internet. *In Intelligent Autonomous Systems 12; Springer: New York, NY, USA, pp.217-225.*
- [4]. Paiva, E.; Gomez-Redondo, M.; Rodas, J. (2019). Cascade First and Second Order Sliding Mode Controller of a QuadRotor UAV based on Exponential Reaching Law and Modified Super-Twisting Algorithm. *In Proceedings of the 2019 Workshop on Research, Education and Development of Unmanned Aerial Systems, IEEE, pp.100-105.*
- [5]. Dierks, T.; Jagannathan, S. (2009). Output feedback control of a quadrotor UAV using neural networks. *IEEE Trans. Neural Netw. Vol.21, pp.50-66.*
- [6]. B. Kada, Y. Ghazzawi. (2011). Robust PID Controller Design for an UAV Flight Control System. *Proceedings of the World Congress on Engineering and Computer Science, Vol. 2, pp.315-319.*
- [7]. Aline Ingabire, Andrey A. Sklyarov. (2019). Control of longitudinal flight dynamics of a fixed-wing UAV using LQR, LQG and nonlinear control. *EEESTS.*
- [8]. Dawn Tilbury. (2017). Aircraft Pitch: System Modeling, the Control Tutorials for MATLAB and Simulink. *The University of Michigan.*
- [9]. Bhar Kisabo Aliyu, Charles Osheku. (2015). Oscillation Analysis for Longitudinal Dynamics of a Fixed-Wing UAV Using PID Control Design. *SCIENCEDOMAIN international, pp 1-13.*